BJR

Received: 24 September 2015 | Revised: 10 February 2016 | Accepted: 2 March 2016

http://dx.doi.org/10.1259/bjr.20150797

Cite this article as:
Van Leeuwen FWB, Valdés-Olmos R, Buckle T, Vidal-Sicart S. Hybrid surgical guidance based on the integration of radionuclear and optical technologies. *Br J Radiol* 2016; **89**: 20150797.

REVIEW ARTICLE

Hybrid surgical guidance based on the integration of radionuclear and optical technologies

[1]FIJS W B VAN LEEUWEN, PhD, [1,2]RENATO VALDÉS-OLMOS, MD, PhD, [1]TESSA BUCKLE, PhD and [3]SERGI VIDAL-SICART, MD, PhD

[1]Interventional Molecular Imaging Laboratory, Department of Radiology, Leiden University Medical Center, Leiden, Netherlands
[2]Department of Nuclear Medicine, Netherlands Cancer Institute–Antoni van Leeuwenhoek, Amsterdam, Netherlands
[3]Nuclear Medicine Department, Hospital Clínic of Barcelona, Barcelona, Spain

Address correspondence to: Dr Fijs W B van Leeuwen
E-mail: *f.w.b.van_leeuwen@lumc.nl*

ABSTRACT

With the evolution of imaging technologies and tracers, the applications for nuclear molecular imaging are growing rapidly. For example, nuclear medicine is increasingly being used to guide surgical resections in complex anatomical locations. Here, a future workflow is envisioned that uses a combination of pre-operative diagnostics, navigation and intraoperative guidance. Radioguidance can provide means for pre-operative and intraoperative identification of "hot" lesions, forming the basis of a virtual data set that can be used for navigation. Luminescence guidance has shown great potential in the intraoperative setting by providing optical feedback, in some cases even in real time. Both of these techniques have distinct drawbacks, which include inaccuracy in areas that contain a background signal (radioactivity) or a limited degree of signal penetration (luminescence). We, and others, have reasoned that hybrid/multimodal approaches that integrate the use of these complementary modalities may help overcome their individual weaknesses. Ultimately, this will lead to advancement of the field of interventional molecular imaging/image-guided surgery. In this review, an overview of clinically applied hybrid surgical guidance technologies is given, whereby the focus is placed on tracers and hardware.

INTRODUCTION

Nuclear medicine is the routine clinical methodology used for non-invasive visualization of molecular features in patients. In order to provide optimal clinical value, nuclear medicine requires the addition of other modalities that help place its findings into context. Hence hybrid approaches provide outcome here; hybrid approaches are a well-accepted means to overcome the limitations of individual technologies and to generate a "best of both worlds" model. A prime example is the hardware-based fusion of nuclear imaging modalities and radiological modalities, such as the fusion of single-photon emission CT (SPECT) or positron emission tomography (PET) with anatomical information provided by CT or MRI.

In image-guided surgery applications such as sentinel node (SN) procedures, a similar approach can be applied. Optical imaging *via* the use of blue dye is often used to complement nuclear medicine-based radioguided surgery,[1–3] and optical imaging based on luminescence imaging can enhance intraoperative visualization. The latter can also help in the accurate demarcation of superficial (<1-cm) lesions in real time.[4] The complementary features of radionuclear and optical imaging modalities ensure that neither can replace the other, and a hybrid approach that combines the two could therefore result in additional information during the intervention.

Hybrid radionuclear/fluorescence imaging can occur using two different tracers, but this increases the risk of discrepancies between the individual findings.[5] This can be prevented by fully integrating the two techniques through the use of dedicated tracers and/or modalities, herein hybrid tracers need to express two (or more) distinct signatures. When designing hybrid tracers, the contrast sensitivity (meaning the amount of moles of contrast required for detection using a specific modality) has to be taken into account. Unfortunately, this sensitivity can vary significantly between modalities.[6,7] For example, the contrast sensitivity of MRI is around 10^{-6} mol and of CT is 10^{-3} mol. In nuclear medicine, however, PET and SPECT scanners have a contrast sensitivity that is high enough to identify quantities as low as 10^{-10}–10^{-15} mol. The difference in sensitivity between nuclear medicine and MRI (up

to 9-orders of magnitude) and CT (up to 12-orders of magnitude) means that, from a chemical perspective, it is difficult to generate hybrid tracers that can be detected with both modalities. Luminescence-based imaging modalities, however, have a sensitivity that is highly similar to the one reported for nuclear medicine techniques, namely 10^{-9}–10^{-12} mol. Hence, hybrid tracers that contain both radiolabels and luminescence labels seem to have most clinical potential. This automatically reflects on the hardware development, by generating a need for modalities that can detect both radionuclear and luminescence signals.

In this review, we discuss the underlying physics behind radionuclide and luminescence-based emissions and extrapolate this to the hybrid surgical guidance concept in the form of hybrid tracers, the need for preoperative imaging, hybrid modalities for surgical guidance and the value of luminescence during pathological evaluation of hybrid tracers. Hereby we focus on the hybrid technologies that have been reported in clinical use, both for benign and malignant lesions. Since most readers already have knowledge on nuclear medicine, we also focused on the added value that luminescence may offer.

Basic physics, radionuclide and luminescence-based emissions

Radionuclide emissions

Most people active in medical imaging are well aware of the strengths and shortcomings of radioactive emissions generated by medical isotopes. In short, during their decay, radioisotopes spontaneously emit a form of radiation, of which the rate is dependent on their independent half-life ($t_{1/2}$). Of the standard radiation emissions, several are used in the clinical setting; namely alpha-emissions (α), beta-emissions (β^+ and β^-) and gamma-emissions (γ). In general, α^- and β^- emissions have a strong tissue interaction, a feature that limits their tissue penetration but allows use in therapeutic settings. For diagnostics, the secondary annihilation of 511-keV γ-emissions (resulting from a β^+-emission) or primary γ-emissions in the 25–300 keV range are predominantly used.[7] Although tissue attenuation is energy dependent, all these emission types allow in-depth detection (>10 cm) in humans (Figure 1).

There are a few examples where β-emissions have been directly used for surgical guidance applications, but these are scarce compared with reports using γ-emissions. The radionuclides that have so far been reported for radioguided surgery are: fluorine-18 (^{18}F), ^{32}P, ^{57}Co, ^{67}Ga, ^{68}Ga, ^{89}Zr, ^{90}Y, technetium-99m (^{99m}Tc), ^{111}In, ^{123}I, ^{124}I, ^{125}I, ^{131}I and ^{201}Tl, of which ^{99m}Tc is the most widely applied radionuclide for this application.[8] Of course, the use of radioisotopes implies exposure to radiation for both the patient and the surgical staff. Although studies have shown that when ^{99m}Tc is used exposure to the radiation does not exceed legal limits,[9] there are clear indications that, in particular, the dose accumulation as a result of using β^+-emitters may be limiting for their use in image-guided surgery applications.[8]

Detection of gamma emission during surgery generally occurs using either gamma probes, which enable acoustic tracing of the radioactive "hot-spot" in real time, or portable gamma-cameras that need some time for data acquisition but can generate images of the surgical field.[10] The emission of γ-rays by an isotope occurs in a random fashion and <360°. Given their limited tissue attenuation, γ-rays coming from different directions may be detected, making it difficult to differentiate between hot-spots and background. For example, half of the γ-rays emitted (<180°) in two dimensions can be detected. Of these <180° γ-rays, only a small portion has originated in a direct line (approximately 90°) between the hot-spot and detector. Unfortunately, it is this fraction that is critical for the accurate identification of individual hot-spots. Using physical collimation, γ-rays that are emitted under an unwanted angle can be

Figure 1. Emissions and their degree of tissue penetration. (a) A schematic representation on the relative ability of radioactive (α-, β- and γ-emissions) and luminescence emissions (Cerenkov luminescence and fluorescence) to penetrate human tissue. (b) Schematics of a phantom setup, where (1) represents a gel-phantom with absorbance properties similar to human tissue and (2) represents a diagonally placed glass rod containing a radioisotope [technetium-99m (^{99m}Tc)] and a fluorescence dye (Cy5). The underlying graph depicts the quantified signal intensities along the dotted line as derived from top-view images (data adapted from Oosterom et al[86] published under the terms of the Creative Common Attribution 4.0 unported license http://creativecommons.org/licenses/by/4.0). The anatomical image was made using the visual body software package (Human Anatomy Atlas v. 3.0.1; Argosy Publishing, Inc., Newton, MA).

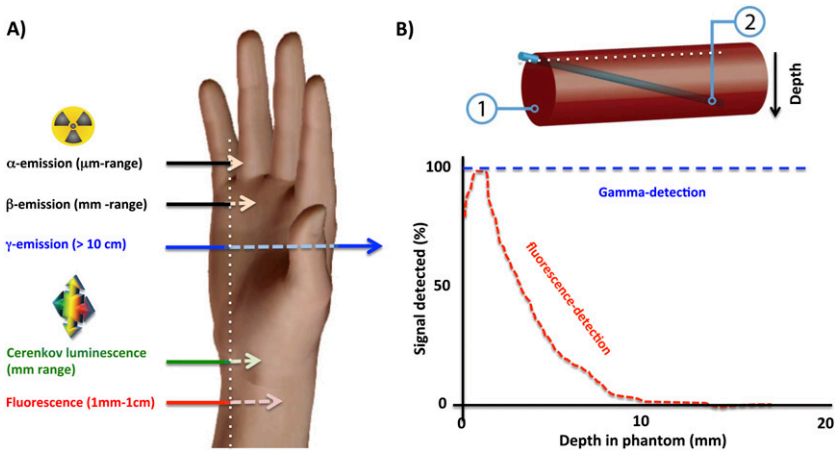

blocked. Although collimation reduces the sensitivity, the specificity and spatial resolution can be improved significantly. In case of annihilation γ-rays, coincidence detection, as used in PET cameras, is used to overcome the requirement of physical collimation. In the last example, electronic collimation is, however, needed to determine the origin of the emission.

Luminescence emissions

Different from radioactive emissions the ins and outs behind using luminescence emissions in a medical setting are often not known. For starters, luminescence is the general term for emission of light by a substance. In the medical setting, fluorescence and Cerenkov luminescence (CL) are the most important types of luminescence used.

For fluorescence, a molecule has to be "excited" by an external light source that matches its absorption optimum. Light absorbance is dependent on the absorbance coefficient, and when efficient, the molecule can be brought into an (unstable) excited state. As soon as the molecule falls back to its stable form, a photon with a wavelength that is longer than that of the absorbed excitation light is emitted. The speed with which this decay occurs (luminescence-lifetime) and the efficiency of the external light conversion (quantum yield) are two additional denominators for the emitted signal. The absorption coefficient as well as the absorption and emission maxima ($\lambda_{ex\,max}$ and $\lambda_{em\,max}$, respectively) may vary for each individual dye.[4] When this process occurs in tissues, there are a number of features that negatively influence accurate detection of the fluorescence signal, namely: (i) reflection of excitation light, (ii) scattering of excitation and emitted fluorescence light, (iii) tissue attenuation/absorbance of both excitation and emitted fluorescence light and (iv) autofluorescence caused by the excitation of endogenous fluorophores. Finally, detection of the fluorescence signal with a light sensitive camera can be hampered by the presence of ambient light or alternative light sources, meaning that the camera system has to be equipped with specific light filters and/or needs to be used under dark conditions. As a result, the signal penetration in real-time applications varies between 0.5 mm and 1 cm, dependent on the wavelength and signal strength of the emission (Figure 1). This said, photons that are emitted from deeper lying structures may still be detected with extended data acquisition times and significantly reduced spatial resolutions.

Uniquely, the decay of β-emitters can induce an optical emission called Cerenkov light. Hereby the energy of a β-particle travelling through a medium induces a weak light emission with a peak intensity in the ultraviolet (<400 nm). This emission spectrum is identical for all β-emitters, but the signal strength increases with the energy of the β-particles, a feature that varies between isotopes.[11,12] Other than with fluorescence, this "spontaneous" type of luminescence emission does not suffer from the limitations that are related to the excitation of a fluorescent dye. Unfortunately, the signal intensity of Cerenkov light is around three orders of magnitude lower than that of fluorescence. Combined with the low peak maximum of the emission ($\lambda_{em\,max} < 200$ nm), this results in limited tissue penetration.[4] By increasing the camera's exposure time, and thus increasing the acquisition time, enough signal can be detected to generate an image. The use of cut-off filters during the data collection process is undesirable in this setting as it will result in a significant loss of signal. Without filters, however, the camera will not be able to differentiate between CL and all other forms of light present in the operating room (*e.g.* ambient light) and light from the devices present. Hence, the use of this technology is best under conditions where the signal of the background light is low enough to allow specific detection of CL.

Luminescence for surgical guidance

When luminescence was initially introduced in surgical guidance procedures, it was hypothesized that the fluorescent dyes used could overcome the need for radioactive tracers, thereby improving logistics and decreasing the radiation exposure to the surgical personnel. However, looking at the physical restraints (see Luminescence section), there simply are some things that luminescence alone cannot achieve. The most important feature herein is the generation of in-depth guidance to unknown locations in the body.

In general, fluorophores that emit in the visible range of the light spectrum (400–650 nm)[13] are used in clinical applications. Non-visual near-infrared (NIR) emissions (750–1000 nm), however, provide a valuable alternative as they benefit from the tissue transparency window that is present at these wavelengths. However, compared with visible and far-red fluorophores, such as Fluorescein ($\lambda_{em\,max}$: around 515 nm) and cyanine 5 (Cy5) ($\lambda_{em\,max}$: around 670 nm), the quantum yield/signal intensity of NIR fluorophores such as indocyanine green (ICG) ($\lambda_{em\,max}$: around 820 nm) is substantially lower. Since this feature is also of influence on the tissue penetration, it balances out the favourable advantages of NIR fluorophores.[14]

For detection of luminescence emissions in a clinical setting, a range of technologies are already commercially available. These range from technologies that acoustically trace luminescence emissions to cameras for open and/or endoscopic interventions.[13,15] Recently, even the use of dedicated surgical binocular goggles that allow for real-time luminescence imaging has been proposed.[16]

Hybrid tracers

As said previously, so-called hybrid tracers can be used in an attempt to integrate radioguidance and fluorescence guidance. This concept is based on a single tracer that can be detected with both modalities. Hybrid tracers can be divided in two distinct classes. The first consists of tracers that contain a fluorescent dye and a radioisotope. This class of compounds is increasingly being studied in a pre-clinical setting, but to date only a limited number of tracers have been successfully translated to the clinic.[13] The second class consists of radiotracers that show β-emissions, which can induce CL emissions. This approach can be used in combination with already clinically applied beta-emitting (β^+ and β^-) radiotracers, but clinical use is still limited owing to technical challenges.[17] In the section below, practical examples regarding the use of both hybrid tracer types in clinical studies are discussed in more detail.

Combined tracers build-up out of a fluorescent dye and a radioisotope

The combination of radioisotopes with fluorescent dyes has the advantage that all components of the tracer (targeting, nuclear

detection or luminescence imaging) can be optimized individually. The radioisotope can be tuned for its compatibility with (surgical) imaging modalities and the dose exposure for both the patient and the surgical personnel,[8] whereas the fluorescent dye can be optimized for its signal intensity (10^{-2}–10^{-1} photons s^{-1} $molecule^{-1}$) and excitation and emission wavelengths (common range 400–900 nm).[4] A potential downside of this approach is that integration of the two labels in a single molecule may yield synthetically complex molecular structures. In addition, each newly developed hybrid tracer has to be translated to the clinical setting individually, which results in the fact that only a few hybrid tracers have been used in patients. Interestingly, the clinically, most widely used hybrid tracers are the product of straightforward synthetic procedures wherein already clinically approved compounds were converted into hybrid tracer analogues.

In its most simplistic form, a fluorescent dye is functionalized with a radioisotope. This concept has been reported for a number of pre-clinically applied dyes; examples are ^{131}I-Hoechst[18] and ^{18}F-boron-dipyrromethene (BODIPY).[19] More importantly, this approach has also been used to convert the clinically used dyes methylene blue (MB) and fluorescein into hybrid tracers.

MB, a dye commonly used for optical visualization of the lymphatic ducts, has been radioiodinated as early as 1992 by Blower et al[20] using standard iodination methods in combination with a variety of radioactive-iodine isotopes (^{123}I, ^{125}I and ^{131}I). Although MB has been predominantly used for the visual contrast it provides with its blue appearance, this dye was later also shown to possess fluorescence properties (λ_{ex} = 670 nm and λ_{em} = 680 nm).[21] The limited quantum yield (2%) of the emission generated by MB requires a highly sensitive luminescence camera.[4] Since suitable fluorescence cameras had yet to be developed at the time these studies using the hybrid MB analogues were performed, this feature was not explored. Initially, radioiodination of MB was purely meant to utilize the tissue-binding properties of MB during radioguidance towards SNs in breast cancer cases. Here, positive visualization was seen in 11 out of 12 patients.[22] Melanoma lesions were visualized in 10 out of 12 primary lesions,[23] and in patients with carcinomia of/lesions in the parathyroid gland one 1 out of 4 lesions was visualized.[20] Although still unclear, uptake of this particular hybrid tracer is thought to be driven by the charged/lipophilic structure of MB. Although some claim that MB binds to the mitochondria, there is only limited overlap between uptake of MB and the mitochondrial radiotracer ^{99m}Tc-sestamibi.[13] A further downside of MB is that the Food and Drug Administration has issued a warning against its use due toxic side effects.

Radiolabelled fluorescein (^{131}I-diiodofluoresceine) was already used in the clinic as early as 1948.[24] At that time, fluorescein provided a clinical tool that enabled assessment of the disruption of the vascular network in malignant brain tumours. In the areas where the blood–brain barrier was disrupted, leakage and subsequent accumulation of the tracer was seen in the surrounding tissue.[25,26] Surgical identification of these areas could then be achieved using highly superficial but visible detection of this fluorescent dye ($\lambda_{ex\,max}$ = 488 nm and $\lambda_{em\,max}$ = 515 nm). With the introduction of radioisotopes, in-depth detection of the same dye was also made possible using a Geiger–Müller tube. Here, overlap in findings obtained with both modalities was seen in 11 out of 12 cases.[25] Alternatively, the radioactive signature was shown to provide accurate pre-operative guidance in 200 out of 536 additional patients.[27]

More recently (2009), a self-assembled hybrid tracer that consists of the clinically approved compounds ICG and ^{99m}Tc-nanocolloid (ICG-^{99m}Tc-nanocolloid) was introduced in the clinic.[28–30] This purposely developed SN tracer exploits the nodal retention of ^{99m}Tc-nanocolloid as well as the near-infrared fluorescence properties of ICG ($\lambda_{ex\,max}$ = 780 nm and $\lambda_{em\,max}$ = 820 nm).[31] Although this hybrid assembly comprises different self-assembled components (being one albumin-colloid and multiple ICG dye molecules), pre-clinical validation as well as a clinical reproducibility study demonstrated that the nodal retention behaviour of ICG-^{99m}Tc-nanocolloid was identical to the nodal retention behaviour of its parental radiotracer ^{99m}Tc-nanocolloid.[32,33]

The *ex vivo* concurrence of both signals reported in numerous clinical studies suggests that dissociation of the two components does not occur in the lymphatics. In contradiction to the other hybrid tracers mentioned above, the hybrid properties of this compound have been evaluated in different centres and in a relatively large and heterogeneous patient population which covers multiple malignancies ($n > 600$ patients). Indications that have been reported are prostate cancer (Figure 2),[30,34] penile cancer,[35] melanoma,[33,36,37] vulvar cancer,[38,39] oral cavity cancer[37,40] and breast cancer.[41] These combined studies have shown that the addition of real-time fluorescence imaging to an otherwise standard radioguidance procedure not only increased the surgeons confidence that he/she was dissecting the intended tissue of interest but also proved valuable during the detection of SNs located close to a high radioactive background source such as the injection site.[40] A direct comparison between the optical identification enabled by a (non-fluorescent) blue dye and that provided by the luminescent component of ICG-^{99m}Tc-nanocolloid indicated that the first detects around 60% of the SNs, whereas the second detects >95% of the SNs.[35–38]

Since the available clinical data provide a strong argument for the use of hybrid tracers, it is likely that efforts focused on applying this concept to tumour biomarker-targeted imaging approaches will also be translated to the clinic. Overviews describing the pre-clinical evaluation of biomarker-specific hybrid tracers have been provided for targeting peptide moieties[42] and antibodies.[43] Interestingly, the first reports of a hybrid labelled antibody against CEA were already presented in 1992. Folli et al[44] used a fluorescein-labelled carcinoembryonic antigen (CEA)-targeted tracer (CEA-mAB-FITC) that was also ^{125}I-radioiodinated to identify colorectal carcinoma. Six patients received 4.5–9.0 mg of CEA-mAB-FITC, and fluorescence imaging was evaluated *in vivo* in one patient. Further fluorescence imaging and scintillation counting was performed *ex vivo* 24 h post-injection. Conjugation with fluorescein reduced the circulation half-life of CEA-mAB; unconjugated antibody showed a half-life of 52 h, whereas fluorescein labelling reduced this to

Figure 2. The hybrid surgical guidance concept. The top line displays a schematic setup that illustrates the hybrid surgical guidance concept. The bottom example depicts the use of indocyanine green–technetium-99m–nanocolloid during robot-assisted SN biopsy in a patient with prostate cancer: single-photon emission CT (SPECT)/CT imaging followed by intraoperative gamma tracing and endoscopic fluorescence imaging. The anatomical image was made using the visual body software package (Human Anatomy Atlas v. 3.0.1; Argosy Publishing, Inc., Newton, MA).

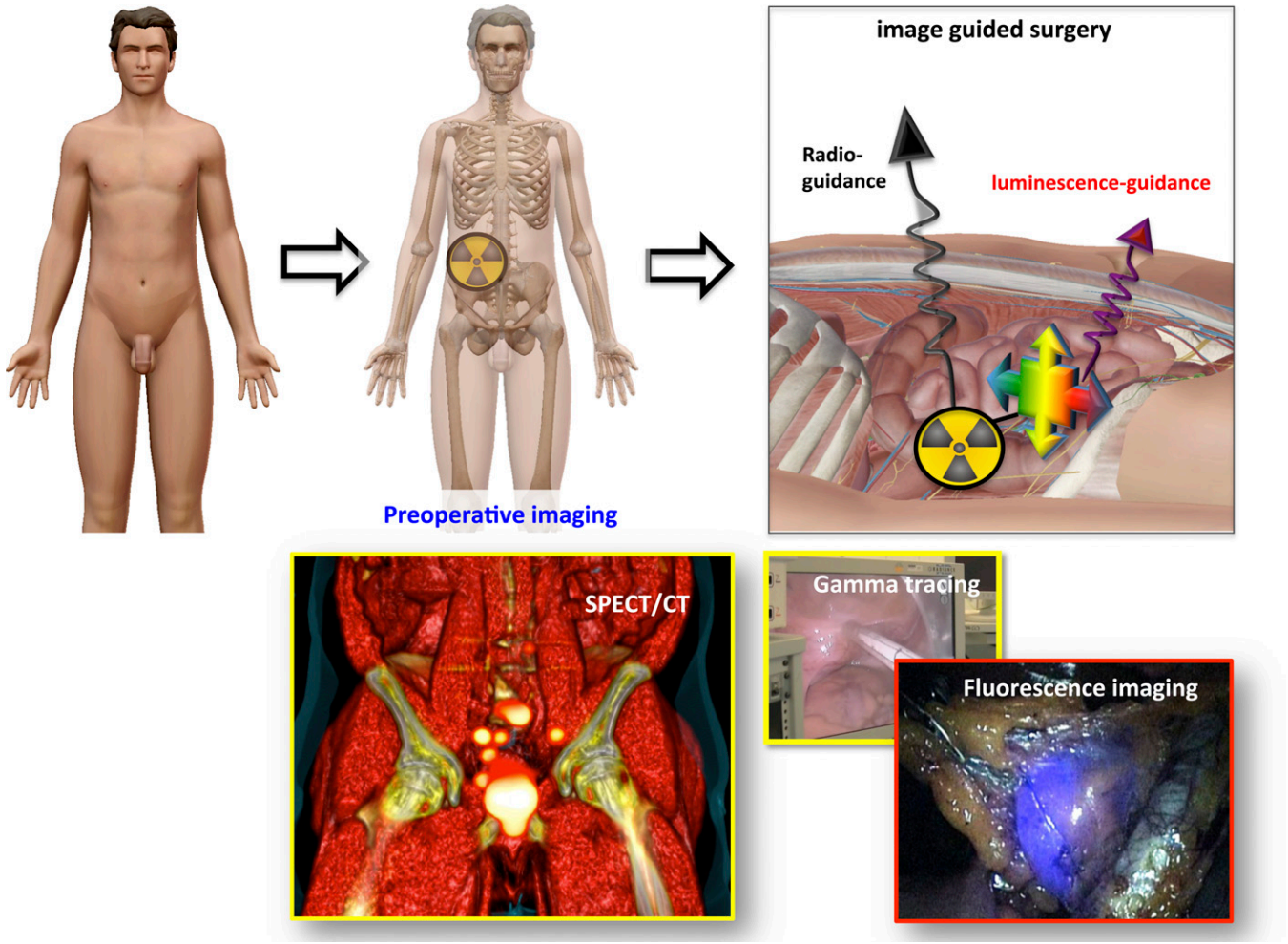

36 h (1 : 10 and 1 : 11 antibody : fluorescein) or even 24 h (1 : 14).[44] More recently, ^{124}I-radioiodinated cRGDY-PEG-C dots (Cy5-containing nanoparticles) were applied in patients.[45] In five patients with metastatic melanoma, 185-MBq ^{124}I-cRGDY-PEG-C dots were administered, and in two (40%) out of the five patients, the ^{124}I-cRGDY-PEG-C dots were able to visualize a lesion on PET/CT. *In vivo* fluorescence imaging was not reported.

Cerenkov

CL ($\lambda_{em\,max} < 200$ nm), a secondary effect induced by β-emissions, was introduced as a biomedical imaging technology in 2009.[11,12] A major advantage of CL is that all β^+- and β^--emitting radioisotopes with an energy >0.21 MeV can potentially be used. This means that existing nuclear medicine applications and imaging approaches can, in theory, be complemented with optical imaging, without requiring the introduction of new tracers.

The efficacy with which CL is induced is limited, yielding a relatively low signal intensity than, *e.g.* the use of ICG (10^{-5} *vs* 10^{-2} photons s^{-1}, respectively).[4] The intensity of CL emission can be increased by using high energy emitters; ^{18}F induces 1.4 photons per decay in water, whereas ^{90}Y induces 57 photons under the same conditions.[46] Given the minimally invasive nature of image-guided surgery procedures in CL, there is a clear clinical preference for radioisotopes that can safely be used for diagnostic purposes, *e.g.* ^{131}I, ^{68}Ga, ^{89}Zr, ^{18}F (half-life of 8 days, 271 days, 78.4 h and 110 min, respectively). Since the amount of β-emission is directly related to the dose and decay half-life of the isotopes used, the time between tracer administration and the initiation of the surgical guidance process directly influences the intensity of CL emission. Using highly light sensitive (bioluminescence) cameras, CL has been explored in multiple pre-clinical settings, using both existing and newly developed tracers.[47–51]

The first, and seemingly promising, results in humans obtained with CL on the visualization of superficially located lesions were reported in 2013. Initially, the thyroid accumulation of a therapeutic dose of ^{131}I (550 MBq) was used to allow for proof-of-

concept CL imaging of the thyroid in a single patient placed in a darkened room.[52] Following routine ^{18}F-fludeoxyglucose (^{18}F-FDG) PET/CT imaging (approximately 450 MBq) CL imaging was successfully used to reveal the site of accumulation in PET-positive lymph nodes in the neck and axilla [four patients with lymphoma ($n = 2$), lung ($n = 1$) or breast ($n = 1$) cancer].[53] CL imaging with ^{18}F-FDG was recently also evaluated *in vivo* in four patients with colorectal cancer.[54]

Pre-operative imaging in the context of hybrid surgical guidance

The emergence of two-dimensional and three-dimensional (3D) nuclear molecular imaging techniques, such as scintigraphy, SPECT and PET, has enabled us to visualize, measure and characterize biological processes in the human body. All these techniques make use of a gamma emission that originates from accumulated radiotracers. As a result of the high sensitivity and specificity of these radiopharmacological tracers, SPECT and PET have proven to be valuable diagnostic tools in oncology. Their value was further strengthened by the integration of these nuclear imaging methods with CT or even MRI; SPECT/CT, PET/CT or PET/MRI modalities have provided precise anatomical localization of the visualized radioactive hot-spots.[55] This concept has helped create road maps for surgical guidance. As stated above, integration of nuclear medicine with MRI at the tracer level does not seem to add value owing to the large difference in detection sensitivities between the modalities.

A typical example where findings in nuclear medicine are used to drive surgical excision are procedures where the spread of disease may be diffuse, *e.g.* SN procedures. Here, the incorporation of SPECT/CT adds a third dimension by incorporating anatomical landmarks that can be recognized intraoperatively.[56] SN-imaging has been validated in breast cancer,[57] melanoma,[58] prostate cancer,[59] gynaecological malignancies[60,61] and other solid tumour types. In a series including 1508 patients, the drainage basin mismatch between SPECT/CT and planar imaging varied from 11% in melanoma to 16.5% in breast cancer and almost 52% in pelvic malignancies.[62] Since the detection rate of SPECT/CT was found to be superior, this led to an adjustment in surgical planning of the SN procedure of 17% for breast cancer, 37% for melanoma and almost 66% for patients with pelvic cancer. In the context of hybrid surgical guidance towards SNs, the use of a 3D imaging modality seems to be critical for pre-operative imaging. The value of hybrid tracers in this concept was demonstrated in a reproducibility study wherein the hybrid tracer ICG-^{99m}Tc-nanocolloid was compared with the parental ^{99m}Tc-nanocolloid.[33] Subsequently, combined pre-operative lymphatic mapping using SPECT/CT and intraoperative radioguidance and fluorescence guidance has been reported for oral cavity cancer ($n = 14$),[40] penile cancer ($n = 65$),[35] vulvar cancer ($n = 15$),[38] prostate cancer ($n = 51$)[30,34] and melanoma ($n = 104$).[36]

Although applied in a somewhat different setup, Maurer et al[63] recently illustrated that a similar concept using PET/MRI combined with a PET tracer that targets the prostate-specific membrane antigen (^{68}Ga-prostate-specific membrane antigen) could be used to direct radioguided surgery using an ^{111}In-labelled derivative of the tracer. One may argue that extension of this concept with luminescence imaging is a logical next step in these developments.

Hybrid surgical guidance modalities

At the moment, most hospitals active in research in the field of image-guided surgery have both gamma-tracing and fluorescence-tracing modalities available for clinical use. Increasingly, these modalities are being applied in parallel. Hence, there is a growing interest in the development of (hybrid) surgical modalities that can be applied for both radioguidance and fluorescence guidance. Although published literature examples are few, most of the initiatives that are out there aim to extend the applicability of traditional γ-ray detection technologies.

The first gamma detectors to be used for radioguided surgery were handheld gamma probes that instantly convert detected gamma counts into acoustic signals that guide the probe to a radioactive hot-spot. The sensitivity of this approach is high, but the spatial resolution is poor. This is especially problematic in areas where lesions are located in close proximity to sites with high background signal such as the injection site. Optical tracing, with a limited in-depth sensitivity but a higher special resolution, could provide outcome here. As far as we know, only one clinically used hybrid device that enables combined radioguidance and fluorescence guidance has been reported on, namely a γ-ray detection probe that was enhanced with acoustic ICG fluorescence-tracing capabilities (the optonuclear probe by EURORAD, Chennevieres/Marne, France; Figure 3a).[15,64] The clinical utility of this optonuclear technology was evaluated in combination with the hybrid tracer ICG-^{99m}Tc-nanocolloid. *Ex vivo* evaluation of 150 SNs revealed that the gamma-tracing option of this probe correctly identified 100% of the samples, and 98.9% of the fluorescent SNs could be identified with fluorescence tracing. Using optimized fluorescence settings, *in vivo* fluorescence tracing allowed for the accurate identification of 20 SNs in 9 patients.

As an alternative to gamma probes, portable gamma cameras have been used to provide imaging data during surgery. The potential benefits of expanding conventional intraoperative gamma detection to include intraoperative imaging include real-time access to imaging information, a larger field of view than a gamma probe can cover and visual assistance in localization and verification of target tissue resection. On the other hand, the intraoperative use of these portable devices might lead to excision of additional SNs.[65] Over the years, these portable cameras have improved significantly; the devices are now able to generate images with a resolution up to 3 mm within 30 s.[66] In some cases, a portable gamma camera was even shown to detect lesions not initially identified with SPECT/CT or lymphoscintigraphy,[67] suggesting that, in theory, such devices can also be used to improve pre-operative SN visualization.[68]

The additional benefit of intraoperative use of a portable gamma camera was demonstrated in a retrospective study involving 754 patients with breast cancer. Until October 2009, excision of the SNs was solely guided by a hand-held gamma probe. After that date, a portable gamma camera was introduced in the operating room. This approach allowed SN identification in 725

Figure 3. Illustration of hybrid modalities in use for surgical guidance. (a) An optonuclear technology that allows for both gamma and fluorescence tracing.[15] (b) The surgical navigation of a fluorescence laparoscope in pre-operative single-photon emission CT (SPECT)/CT images.[79]

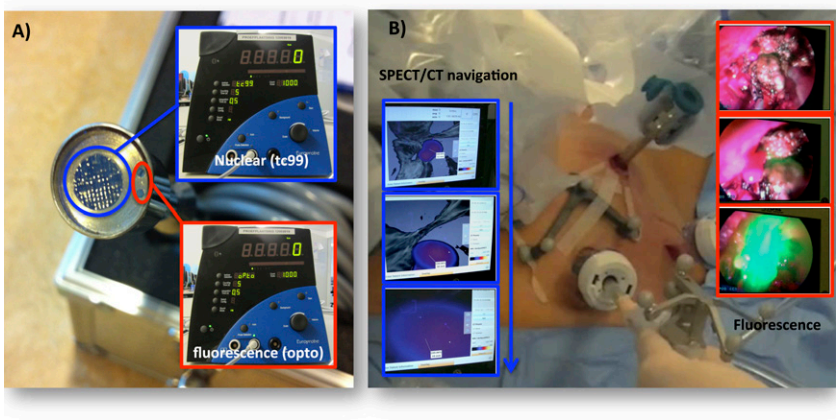

out of the 754 patients studied (global effectiveness was 96.2%). Interestingly, there was a significant difference in the SN identification before and after the incorporation of the portable gamma camera of 4.6% (95% CI of the difference 2–7.2%, $p = 0.0037$).[69] In patients with melanoma, similar advantages were seen.[70] Important to note is that in cases where there are multiple radioactive nodes or when the SN is located near or directly beside the injection site, the use of portable gamma cameras may help reduce the surgical time.[71–74]

Given the successful hybrid extension of the gamma probe technology, one may reason that the same, or a similar approach, may also be of value for a portable gamma camera.[10] However, as far as we know, such a combination has not yet been reported in clinical literature. What has been proposed/evaluated by different groups are gamma cameras equipped with white light imaging options that help place the radioactive hotspots into anatomical context. This approach could aid the lesion localization and should hereby help overcome orientation problems. Such a concept was successfully evaluated using a Sentinella (Oncovision, Valencia, Spain) platform that was equipped with an optical module. This study was performed in a multicentre setup that included 25 patients (12 melanoma, 2 oral cavity and 11 breast cancer) and only showed an error in optical image co-registration of between 0 and 2.0 cm.[75] More recently, Ng et al[76] applied a different concept to a small field-of-view gamma camera and tested this in a phantom setup. Theoretically, a similar system comprising of a fluorescence excitation source and camera would allow fully integrated gamma and fluorescence imaging using a single device.

To further advance the γ-ray-based radioguided surgery concept, an intraoperative freehand SPECT technology was introduced (declipseSPECT®; SurgicEye GmbH, Munich, Germany). The sensitivity and resolution of this system is restricted by the surgical modality used to generate the freehand SPECT images, which can either be a gamma probe[77] or a gamma camera.[78] Through the use of fiducial markers on the patient and the gamma-tracing/imaging modality, both can be tracked relative to each other. This results in a 3D image that can be overlaid on the patient position (augmented reality) and can be used for the virtual navigation of surgical tools (Figure 3). The same system can be used to load pre-operative SPECT/CT images and use these for navigation purposes.[79]

Logically, one may also make use of a virtual nuclear navigation technology to guide, *e.g.* a fluorescence camera/endoscope, using pre-operative imaging information, to the area harbouring a hybrid tracer.[80] Although only a single patient was reported, the first clinical results underlined that it was possible to intraoperatively guide the tip of a fluorescence laparoscope to radioactive hot-spots defined on SPECT/CT, in a setup similar to the phantom studies.[81] This said, movement artefacts between pre-operative imaging and the surgical setting proved to be a limiting factor, something that may be overcome when intraoperatively acquired freehand SPECT is used as basis for navigation rather than pre-operative imaging information.[82]

Pathological examination

Next to providing a valuable addition to surgical guidance procedures, the hybrid concept also has potential during (pathological) tissue examination. Here, optical signals can be used to relate the tracer accumulation to the tumour margins. In the pre-clinical setting, the concept has been applied for both fluorescence and CL.[48,83] Given the limited use of hybrid tracers in a clinical setting, such extensions into (molecular) pathology are a lot less common in human studies.

Using the hybrid tracer ICG-^{99m}Tc-nanocolloid, sites of tracer deposition and accumulation in SNs could be demonstrated (Figure 4). The first feature allowed establishment of the relationship between the site of tracer deposition and the lymphatic drainage of prostate cancer.[84] The second feature, accumulation in SNs, revealed that there is no clear relationship between nodal tumour presence and the accumulation of a SN tracer.[35] One may reason that similar to the fluorescence-based validation work performed preclinically with receptor-targeted fluorescent imaging agents,[85] the same concept can in the future be used in combination with clinically applied receptor-targeted hybrid tracers.

Figure 4. The use of fluorescence in *ex vivo*/pathological specimens and cells. (a) An example that illustrates how indocyanine green–technetium-99m–nanocolloid (ICG-^{99m}Tc-nanocolloid) deposits (in rainbow) are distributed throughout the prostate in relation to the tumour distribution (dotted line: adapted from Buckle et al[84] with permission form the Society of Nuclear Medicine and Molecular Imaging Inc.). (b) Microscopic imaging of ICG-^{99m}Tc-nanocolloid uptake in a sentinel node: fluorescence (green) and relative to the tumour distribution (black line: adapted from Brouwer et al[35] with permission from Elsevier). (c) Confocal image of Cy5-nanocolloid (blue) in human macrophages.

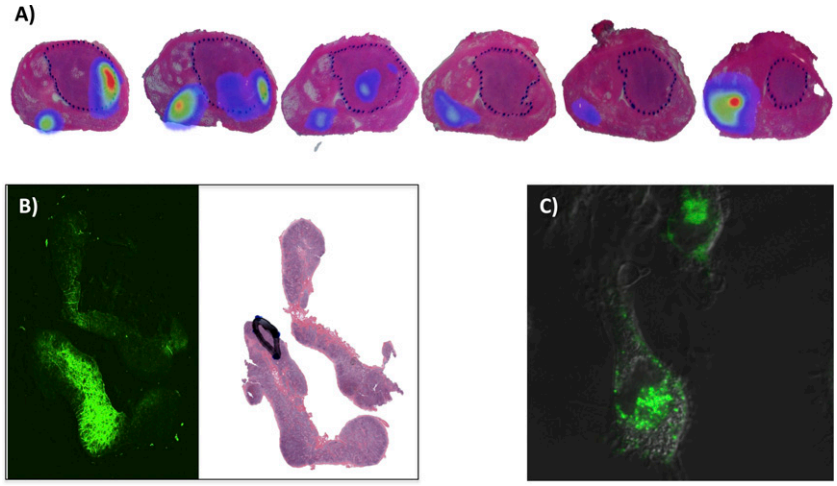

Another emerging application of hybrid tracing in *ex vivo* surgical specimens is based on Cerenkov imaging. Using a black-box camera in the operating room, a group from Kings College London, London, UK, has been able to address the tracer distribution in *ex vivo* surgical specimens.[87] Such a technology may in future allow for intraoperative confirmation of tumour-free surgical margins.

CONCLUSIONS

The emergence of hybrid tracers that facilitate both nuclear and luminescence imaging has provided a first step in the clinical integration of these powerful interventional molecular imaging technologies. Early results indicate that in a hybrid setup, luminescence technologies have the potential to complement nuclear medicine and can even act in synergy. Some of the most important features are listed below:

– The use of a hybrid tracer prevents discrepancies between pre- and intraoperative imaging. Hereby pre-operative imaging data can be used to facilitate navigation;
– The radioactive component of a hybrid tracer helps to identify distant and aberrant sites of interest on a macroscopic scale while the luminescent component allows for more microscopic identification of lesions and their margins, both *in vivo* and *ex vivo*;
– The limited tissue penetration of luminescence signals is a weakness of the technology but at the same time is of value when lesions are located close to high background signals (*e.g.* injection site);
– Similar to the blue dye, luminescence imaging can be used to provide real-time, but superficial, surgical guidance.

Early clinical studies have already demonstrated that hybrid tracers can preserve the more traditional nuclear medicine imaging procedures while improving surgical guidance *via* the use of luminescence. These initial successes are now also reflecting in the engineering of hybrid modalities for surgical guidance.

FUNDING

We acknowledge the European Research Council under the European Union's Seventh Framework Program (FP7/2007-2013)/ERC grant agreement no. 2012-306890; a Koningin Wilhelmina Fonds translational research award (Grant No. PGF 2009-4344); The Netherlands Organization for Scientific Research (NWO; STW BGT 11272); and the 2015–2016 Postdoctoral Molecular Imaging Scholar Program Grant granted by the Society of Nuclear Medicine and Molecular Imaging and the Education and Research Foundation for Nuclear Medicine and Molecular Imaging for support.

REFERENCES

1. Amersi F, Hansen NM. The benefits and limitations of sentinel lymph node biopsy. *Curr Treat Options Oncol* 2006; **7**: 141–51. doi: http://dx.doi.org/10.1007/s11864-006-0049-y
2. Nieweg OE, Estourgie SH, van Rijk MC, Kroon BB. Rationale for superficial injection techniques in lymphatic mapping in breast cancer patients. *J Surg Oncol* 2004; **87**: 153–6. doi: http://dx.doi.org/10.1002/jso.20108
3. Bluemel C, Herrmann K, Giammarile F, Nieweg OE, Dubreuil J, Testori A, et al. EANM practice guidelines for lymphoscintigraphy and sentinel lymph node biopsy in melanoma. *Eur J Nucl Med Mol Imaging* 2015; **42**: 1750–66. doi: http://dx.doi.org/10.1007/s00259-015-3135-1
4. Chin PT, Welling MM, Meskers SC, Valdes Olmos RA, Tanke H, van Leeuwen FW.

Optical imaging as an expansion of nuclear medicine: Cerenkov-based luminescence *vs* fluorescence-based luminescence. *Eur J Nucl Med Mol Imaging* 2013; **40**: 1283–91. doi: http://dx.doi.org/10.1007/s00259-013-2408-9

5. van Leeuwen FW, van der Poel HG. Surgical guidance in prostate cancer: "from molecule to man" translations. *Clin Cancer Res* 2015. Epub ahead of print. doi: http://dx.doi.org/10.1158/1078-0432.CCR-15-2575
6. Meikle SR, Kench P, Kassiou M, Banati RB. Small animal SPECT and its place in the matrix of molecular imaging technologies. *Phys Med Biol* 2005; **50**: R45–61. doi: http://dx.doi.org/10.1088/0031-9155/50/22/R01
7. Povoski SP, Neff RL, Mojzisik CM, O'Malley DM, Hinkle GH, Hall NC, et al. A comprehensive overview of radioguided surgery using gamma detection probe technology. *World J Surg Oncol* 2009; **7**: 11. doi: http://dx.doi.org/10.1186/1477-7819-7-11
8. Bunschoten A, van den Berg NS, Valdés Olmos RA, Blokland JAK, van Leeuwen FWB. Tracers applied in radioguided surgery. In: Herrmann K, Nieweg OE, Povoski SP, eds. *Radioguided surgery—current applications and innovative directions in clinical practice*. Switzerland: Springer International Publishing; 2015. pp. 75–101.
9. Sera T, Mohos G, Papos M, Osvay M, Varga J, Lazar M, et al. Sentinel node detection in malignant melanoma patients: radiation safety considerations. *Dermatol Surg* 2003; **29**: 141–5.
10. Tsuchimochi M, Hayama K. Intraoperative gamma cameras for radioguided surgery: technical characteristics, performance parameters, and clinical applications. *Phys Med* 2013; **29**: 126–38. doi: http://dx.doi.org/10.1016/j.ejmp.2012.05.002
11. Robertson R, Germanos MS, Li C, Mitchell GS, Cherry SR, Silva MD. Optical imaging of Cerenkov light generation from positron-emitting radiotracers. *Phys Med Biol* 2009; **54**: N355–65. doi: http://dx.doi.org/10.1088/0031-9155/54/16/N01
12. Gill RK, Mitchell GS, Cherry SR. Computed Cerenkov luminescence yields for radionuclides used in biology and medicine. *Phys Med Biol* 2015; **60**: 4263–80. doi: http://dx.doi.org/10.1088/0031-9155/60/11/4263
13. van Leeuwen FW, Hardwick JC, van Erkel AR. Luminescence-based imaging approaches in the field of interventional molecular imaging. *Radiology* 2015; **276**: 12–29. doi: http://dx.doi.org/10.1148/radiol.2015132698
14. Chin PT, Beekman CA, Buckle T, Josephson L, van Leeuwen FW. Multispectral visualization of surgical safety-margins using fluorescent marker seeds. *Am J Nucl Med Mol Imaging* 2012; **2**: 151–62.
15. van den Berg NS, Simon H, Kleinjan GH, Engelen T, Bunschoten A, Welling MM, et al. First-in-human evaluation of a hybrid modality that allows combined radio- and (near-infrared) fluorescence tracing during surgery. *Eur J Nucl Med Mol Imaging* 2015; **42**: 1639–47. doi: http://dx.doi.org/10.1007/s00259-015-3109-3
16. Mondal SB, Gao S, Zhu N, Sudlow GP, Liang K, Som A, et al. Binocular Goggle Augmented Imaging and Navigation System provides real-time fluorescence image guidance for tumor resection and sentinel lymph node mapping. *Sci Rep* 2015; **5**: 12117. doi: http://dx.doi.org/10.1038/srep12117
17. Das S, Thorek DL, Grimm J. Cerenkov imaging. *Adv Cancer Res* 2014; **124**: 213–34. doi: http://dx.doi.org/10.1016/B978-0-12-411638-2.00006-9
18. Harapanhalli RS, Howell RW, Rao DV. Bisbenzimidazole dyes, Hoechst 33258 and Hoechst 33342: radioiodination, facile purification and subcellular distribution. *Nucl Med Biol* 1994; **21**: 641–7. doi: http://dx.doi.org/10.1016/0969-8051(94)90030-2
19. Li Z, Lin TP, Liu S, Huang CW, Hudnall TW, Gabbai FP, et al. Rapid aqueous [18F]-labeling of a bodipy dye for positron emission tomography/fluorescence dual modality imaging. *Chem Commun (Camb)* 2011; **47**: 9324–6. doi: http://dx.doi.org/10.1039/c1cc13089g
20. Blower PJ, Kettle AG, O'Doherty MJ, Collins RE, Coakley AJ. 123I-methylene blue: an unsatisfactory parathyroid imaging agent. *Nucl Med Commun* 1992; **13**: 522–7. doi: http://dx.doi.org/10.1097/00006231-199207000-00007
21. Chu M, Wan Y. Sentinel lymph node mapping using near-infrared fluorescent methylene blue. *J Biosci Bioeng* 2009; **107**: 455–9. doi: http://dx.doi.org/10.1016/j.jbiosc.2008.11.011
22. Cundiff JD, Wang YZ, Espenan G, Maloney T, Camp A, Lazarus L, et al. A phase I/II trial of 125I methylene blue for one-stage sentinel lymph node biopsy. *Ann Surg* 2007; **245**: 290–6. doi: http://dx.doi.org/10.1097/01.sla.0000242712.74502.72
23. Link EM, Blower PJ, Costa DC, Lane DM, Lui D, Brown RS, et al. Early detection of melanoma metastases with radioiodinated methylene blue. *Eur J Nucl Med* 1998; **25**: 1322–9. doi: http://dx.doi.org/10.1007/s002590050302
24. Moore GE. Use of radioactive diiodofluorescein in the diagnosis and localization of brain tumors. *Science* 1948; **107**: 569–71. doi: http://dx.doi.org/10.1126/science.107.2787.569
25. Moore GE. Fluorescein as an agent in the differentiation of normal and malignant tissues. *Science* 1947; **106**: 130–1. doi: http://dx.doi.org/10.1126/science.106.2745.130-a
26. Moore GE, Kohl DA, Marvin JF, Wang JC, Caudill CM. Biophysical studies of methods utilizing fluorescein and its derivatives to diagnose brain tumors. *Radiology* 1950; **55**: 344–62. doi: http://dx.doi.org/10.1148/55.3.344
27. Ashkenazy M, Davis L, Martin J. An evaluation of the technic and results of the radioactive di-iodo-fluorescein test for the localization of intracranial lesions. *J Neurosurg* 1951; **8**: 300–14. doi: http://dx.doi.org/10.3171/jns.1951.8.3.0300
28. Buckle T, Chin PT, van Leeuwen FW. (Non-targeted) radioactive/fluorescent nanoparticles and their potential in combined pre- and intraoperative imaging during sentinel lymph node resection. *Nanotechnology* 2010; **21**: 482001. doi: http://dx.doi.org/10.1088/0957-4484/21/48/482001
29. van Leeuwen AC, Buckle T, Bendle G, Vermeeren L, Valdes Olmos R, van de Poel HG, et al. Tracer-cocktail injections for combined pre- and intraoperative multimodal imaging of lymph nodes in a spontaneous mouse prostate tumor model. *J Biomed Opt* 2011; **16**: 016004. doi: http://dx.doi.org/10.1117/1.3528027
30. van der Poel HG, Buckle T, Brouwer OR, Valdes Olmos RA, van Leeuwen FW. Intraoperative laparoscopic fluorescence guidance to the sentinel lymph node in prostate cancer patients: clinical proof of concept of an integrated functional imaging approach using a multimodal tracer. *Eur Urol* 2011; **60**: 826–33. doi: http://dx.doi.org/10.1016/j.eururo.2011.03.024
31. Van Den Berg NS, Buckle T, Kleinjan GI, Klop WM, Horenblas S, Van Der Poel HG, et al. Hybrid tracers for sentinel node biopsy. *Q J Nucl Med Mol Imaging* 2014; **58**: 193–206.
32. Buckle T, van Leeuwen AC, Chin PT, Janssen H, Muller SH, Jonkers J, et al. A self-assembled multimodal complex for combined pre- and intraoperative imaging of the sentinel lymph node. *Nanotechnology* 2010; **21**: 355101. doi: http://dx.doi.org/10.1088/0957-4484/21/35/355101
33. Brouwer OR, Buckle T, Vermeeren L, Klop WM, Balm AJ, van der Poel HG, et al. Comparing the hybrid fluorescent-radioactive tracer indocyanine green-99mTc-nanocolloid with 99mTc-nanocolloid for sentinel node identification: a validation study using lymphoscintigraphy and SPECT/CT. *J Nucl Med* 2012; **53**: 1034–40. doi: http://dx.doi.org/10.2967/jnumed.112.103127
34. KleinJan GH, van den Berg NS, Brouwer OR, de Jong J, Acar C, Wit EM, et al.

Optimisation of fluorescence guidance during robot-assisted laparoscopic sentinel node biopsy for prostate cancer. *Eur Urol* 2014; **66**: 991–8. doi: http://dx.doi.org/10.1016/j.eururo.2014.07.014

35. Brouwer OR, van den Berg NS, Mathéron HM, van der Poel HG, van Rhijn BW, Bex A, et al. A hybrid radioactive and fluorescent tracer for sentinel node biopsy in penile carcinoma as a potential replacement for blue dye. *Eur Urol* 2014; **65**: 600–9. doi: http://dx.doi.org/10.1016/j.eururo.2013.11.014
36. van den Berg NS, Brouwer OR, Schaafsma BE, Mathéron HM, Klop WM, Balm AJ, et al. Multimodal surgical guidance during sentinel node biopsy for melanoma: combined gamma tracing and fluorescence imaging of the sentinel node through use of the hybrid tracer indocyanine green-(99m)Tc-Nanocolloid. *Radiology* 2015; **275**: 521–9. doi: http://dx.doi.org/10.1148/radiol.14140322
37. Stoffels I, Leyh J, Pöppel T, Schadendorf D, Klode J. Evaluation of a radioactive and fluorescent hybrid tracer for sentinel lymph node biopsy in head and neck malignancies: prospective randomized clinical trial to compare ICG-(99m)Tc-nanocolloid hybrid tracer *versus* (99m)Tc-nanocolloid. *Eur J Nucl Med Mol Imaging* 2015; **42**: 1631–8. doi: http://dx.doi.org/10.1007/s00259-015-3093-7
38. Mathéron HM, van den Berg NS, Brouwer OR, Kleinjan GH, van Driel WJ, Trum JW, et al. Multimodal surgical guidance towards the sentinel node in vulvar cancer. *Gynecol Oncol* 2013; **131**: 720–5. doi: http://dx.doi.org/10.1016/j.ygyno.2013.09.007
39. Verbeek FP, Tummers QR, Rietbergen DD, Peters AA, Schaafsma BE, van de Velde CJ, et al. Sentinel lymph node biopsy in vulvar cancer using combined radioactive and fluorescence guidance. *Int J Gynecol Cancer* 2015; **25**: 1086–93. doi: http://dx.doi.org/10.1097/IGC.0000000000000419
40. van den Berg NS, Brouwer OR, Klop WM, Karakullukcu B, Zuur CL, Tan IB, et al. Concomitant radio- and fluorescence-guided sentinel lymph node biopsy in squamous cell carcinoma of the oral cavity using ICG-(99m)Tc-nanocolloid. *Eur J Nucl Med Mol Imaging* 2012; **39**: 1128–36. doi: http://dx.doi.org/10.1007/s00259-012-2129-5
41. Schaafsma BE, Verbeek FP, Rietbergen DD, van der Hiel B, van der Vorst JR, Liefers GJ, et al. Clinical trial of combined radio- and fluorescence-guided sentinel lymph node biopsy in breast cancer. *Br J Surg* 2013; **100**: 1037–44. doi: http://dx.doi.org/10.1002/bjs.9159
42. Kuil J, Velders AH, van Leeuwen FW. Multimodal tumor-targeting peptides functionalized with both a radio- and a fluorescent label. *Bioconjug Chem* 2010; **21**: 1709–19. doi: http://dx.doi.org/10.1021/bc100276j
43. Azhdarinia A, Ghosh P, Ghosh S, Wilganowski N, Sevick-Muraca EM. Dual-labeling strategies for nuclear and fluorescence molecular imaging: a review and analysis. *Mol Imaging Biol* 2012; **14**: 261–76. doi: http://dx.doi.org/10.1007/s11307-011-0528-9
44. Folli S, Wagniéres G, Pélegrin A, Calmes JM, Braichotte D, Buchegger F, et al. Immunophotodiagnosis of colon carcinomas in patients injected with fluoresceinated chimeric antibodies against carcinoembryonic antigen. *Proc Natl Acad Sci U S A* 1992; **89**: 7973–7. doi: http://dx.doi.org/10.1073/pnas.89.17.7973
45. Phillips E, Penate-Medina O, Zanzonico PB, Carvajal RD, Mohan P, Ye Y, et al. Clinical translation of an ultrasmall inorganic optical-PET imaging nanoparticle probe. *Sci Transl Med* 2014; **6**: 260ra149. doi: http://dx.doi.org/10.1126/scitranslmed.3009524
46. Mitchell GS, Gill RK, Boucher DL, Li C, Cherry SR. *In vivo* Cerenkov luminescence imaging: a new tool for molecular imaging. *Philos Trans A Math Phys Eng Sci* 2011; **369**: 4605–19. doi: http://dx.doi.org/10.1098/rsta.2011.0271
47. Xu Y, Chang E, Liu H, Jiang H, Gambhir SS, Cheng Z. Proof-of-concept study of monitoring cancer drug therapy with cerenkov luminescence imaging. *J Nucl Med* 2012; **53**: 312–17. doi: http://dx.doi.org/10.2967/jnumed.111.094623
48. Lohrmann C, Zhang H, Thorek DL, Desai P, Zanzonico PB, O'Donoghue J, et al. Cerenkov luminescence imaging for radiation dose calculation of a ^{90}Y-labeled gastrin-releasing peptide receptor antagonist. *J Nucl Med* 2015; **56**: 805–11. doi: http://dx.doi.org/10.2967/jnumed.114.149054
49. Holland JP, Normand G, Ruggiero A, Lewis JS, Grimm J. Intraoperative imaging of positron emission tomographic radiotracers using Cerenkov luminescence emissions. *Mol Imaging* 2011; **10**: 177–86, 1–3.
50. Hu Z, Qu Y, Wang K, Zhang X, Zha J, Song T, et al. *In vivo* nanoparticle-mediated radiopharmaceutical-excited fluorescence molecular imaging. *Nat Commun* 2015; **6**: 7560. doi: http://dx.doi.org/10.1038/ncomms8560
51. Kotagiri N, Sudlow GP, Akers WJ, Achilefu S. Breaking the depth dependency of phototherapy with Cerenkov radiation and low-radiance-responsive nanophotosensitizers. *Nat Nanotechnol* 2015; **10**: 370–9. doi: http://dx.doi.org/10.1038/nnano.2015.17
52. Spinelli AE, Ferdeghini M, Cavedon C, Zivelonghi E, Calandrino R, Fenzi A, et al. First human Cerenkography. *J Biomed Opt* 2013; **18**: 20502. doi: http://dx.doi.org/10.1117/1.JBO.18.2.020502
53. Thorek DL, Riedl CC, Grimm J. Clinical Cerenkov luminescence imaging of (18)F-FDG. *J Nucl Med* 2014; **55**: 95–8. doi: http://dx.doi.org/10.2967/jnumed.113.127266
54. Hu H, Cao X, Kang F, Wang M, Lin Y, Liu M, et al. Feasibility study of novel endoscopic Cerenkov luminescence imaging system in detecting and quantifying gastrointestinal disease: first human results. *Eur Radiol* 2015; **25**: 1814–22. doi: http://dx.doi.org/10.1007/s00330-014-3574-2
55. Estorch M, Carrio I. Future challenges of multimodality imaging. *Recent Results Cancer Res* 2013; **187**: 403–15. doi: http://dx.doi.org/10.1007/978-3-642-10853-2_14
56. Valdés Olmos RA, Rietbergen DD, Vidal-Sicart S, Manca G, Giammarile F, Mariani G. Contribution of SPECT/CT imaging to radioguided sentinel lymph node biopsy in breast cancer, melanoma, and other solid cancers: from "open and see" to "see and open". *Q J Nucl Med Mol Imaging* 2014; **58**: 127–39.
57. van der Ploeg IM, Nieweg OE, Kroon BB, Rutgers EJ, Baas-Vrancken Peeters MJ, Vogel WV, et al. The yield of SPECT/CT for anatomical lymphatic mapping in patients with breast cancer. *Eur J Nucl Med Mol Imaging* 2009; **36**: 903–9. doi: http://dx.doi.org/10.1007/s00259-008-1050-4
58. Stoffels I, Boy C, Pöppel T, Kuhn J, Klötgen K, Dissemond J, et al. Association between sentinel lymph node excision with or without preoperative SPECT/CT and metastatic node detection and disease-free survival in melanoma. *JAMA* 2012; **308**: 1007–14. doi: http://dx.doi.org/10.1001/2012.jama.11030
59. Vermeeren L, Valdés Olmos RA, Meinhardt W, Bex A, van der Poel HG, Vogel WV, et al. Value of SPECT/CT for detection and anatomic localization of sentinel lymph nodes before laparoscopic sentinel node lymphadenectomy in prostate carcinoma. *J Nucl Med* 2009; **50**: 865–70. doi: http://dx.doi.org/10.2967/jnumed.108.060673
60. Belhocine TZ, Prefontaine M, Lanvin D, Bertrand M, Rachinsky I, Ettler H, et al. Added-value of SPECT/CT to lymphatic mapping and sentinel lymphadenectomy in gynaecological cancers. *Am J Nucl Med Mol Imaging* 2013; **3**: 182–93.
61. Perissinotti A, Paredes P, Vidal-Sicart S, Torné A, Albela S, Navales I, et al. Use of SPECT/CT for improved sentinel lymph node localization in endometrial cancer. *Gynecol Oncol* 2013; **129**: 42–8. doi: http://dx.doi.org/10.1016/j.ygyno.2013.01.022
62. Jimenez-Heffernan A, Ellmann A, Sado H, Huić D, Bal C, Parameswaran R, et al. Results

of a prospective multicenter International Atomic Energy Agency sentinel node trial on the value of SPECT/CT over planar imaging in various malignancies. *J Nucl Med* 2015; **56**: 1338–44. doi: http://dx.doi.org/10.2967/jnumed.114.153643

63. Maurer T, Weirich G, Schottelius M, Weineisen M, Frisch B, Okur A, et al. Prostate-specific membrane antigen-radioguided surgery for metastatic lymph nodes in prostate cancer. *Eur Urol* 2015; **68**: 530–4. doi: http://dx.doi.org/10.1016/j.eururo.2015.04.034
64. Tellier F, Ravelo R, Simon H, Chabrier R, Steibel J, Poulet P. Sentinel lymph node detection by an optical method using scattered photons. *Biomed Opt Express* 2010; **1**: 902–10. doi: http://dx.doi.org/10.1364/BOE.1.000902
65. Vermeeren L, Valdés Olmos RA, Klop WM, Balm AJ, van den Brekel MW. A portable gamma-camera for intraoperative detection of sentinel nodes in the head and neck region. *J Nucl Med* 2010; **51**: 700–3. doi: http://dx.doi.org/10.2967/jnumed.109.071407
66. Hellingman D, de Wit-van der Veen LJ, Klop WM, Olmos RA. Detecting near-the-injection-site sentinel nodes in head and neck melanomas with a high-resolution portable gamma camera. *Clin Nucl Med* 2015; **40**: e11–16. doi: http://dx.doi.org/10.1097/RLU.0000000000000370
67. Vidal-Sicart S, Brouwer OR, Mathéron HM, Bing Tan I, Valdés-Olmos RA. Sentinel node identification with a portable gamma camera in a case without visualization on conventional lymphoscintigraphy and SPECT/CT. *Rev Esp Med Nucl Imagen Mol* 2013; **32**: 203–4. doi: http://dx.doi.org/10.1016/j.remn.2012.06.008
68. Giammarile F, Alazraki N, Aarsvold JN, Audisio RA, Glass E, Grant SF, et al. The EANM and SNMMI practice guideline for lymphoscintigraphy and sentinel node localization in breast cancer. *Eur J Nucl Med Mol Imaging* 2013; **40**: 1932–47. doi: http://dx.doi.org/10.1007/s00259-013-2544-2
69. Goñi Gironés E, Vicente García F, Serra Arbeloa P, Estébanez Estébanez C, Calvo Benito A, Rodrigo Rincón I, et al. Evaluation of the efficacy of sentinel node detection in breast cancer: chronological course and influence of the incorporation of an intraoperative portable gamma camera. [Spanish.] *Rev Esp Med Nucl Imagen Mol* 2013; **32**: 343–9. doi: http://dx.doi.org/10.1016/j.remn.2013.02.008
70. Peral Rubio F, de La Riva P, Moreno-Ramirez D, Ferrandiz-Pulido L. Portable gamma camera guidance in sentinel lymph node biopsy: prospective observational study of consecutive cases. *Actas Dermosifiliogr* 2015; **106**: 408–14. doi: http://dx.doi.org/10.1016/j.ad.2014.11.013
71. Scopinaro F, Tofani A, di Santo G, Di Pietro B, Lombardi A, Lo Russo M, et al. High-resolution, hand-held camera for sentinel-node detection. *Cancer Biother Radiopharm* 2008; **23**: 43–52. doi: http://dx.doi.org/10.1089/cbr.2007.364
72. Paredes P, Vidal-Sicart S, Zanón G, Roé N, Rubí S, Lafuente S, et al. Radioguided occult lesion localisation in breast cancer using an intraoperative portable gamma camera: first results. *Eur J Nucl Med Mol Imaging* 2008; **35**: 230–5. doi: http://dx.doi.org/10.1007/s00259-007-0640-x
73. Bricou A, Duval MA, Bardet L, Benbara A, Moreaux G, Lefebvre F, et al. Is there a role for a handheld gamma camera (TReCam) in the SNOLL breast cancer procedure? *Q J Nucl Med Mol Imaging* 2015. Epub ahead of print.
74. Bricou A, Duval MA, Charon Y, Barranger E. Mobile gamma cameras in breast cancer care—a review. *Eur J Surg Oncol* 2013; **39**: 409–16. doi: http://dx.doi.org/10.1016/j.ejso.2013.02.008
75. Hellingman D, Vidal-Sicart S, de Wit-van der Veen LJ, Paredes P, Valdes Olmos RA. A new portable hybrid camera for fused optical and scintigraphic imaging: first clinical experiences. *Clin Nucl Med* 2016; **41**: e39–43. doi: http://dx.doi.org/10.1097/RLU.0000000000000874
76. Ng AH, Clay D, Blackshaw PE, Bugby SL, Morgan PS, Lees JE, et al. Assessment of the performance of small field of view gamma cameras for sentinel node imaging. *Nucl Med Commun* 2015; **36**: 1134–42. doi: http://dx.doi.org/10.1097/MNM.0000000000000377
77. Wendler T, Herrmann K, Schnelzer A, Lasser T, Traub J, Kutter O, et al. First demonstration of 3-D lymphatic mapping in breast cancer using freehand SPECT. *Eur J Nucl Med Mol Imaging* 2010; **37**: 1452–61. doi: http://dx.doi.org/10.1007/s00259-010-1430-4
78. Engelen T, Winkel BM, Rietbergen DD, KleinJan GH, Vidal-Sicart S, Olmos RA, et al. The next evolution in radioguided surgery: breast cancer related sentinel node localization using a freehandSPECT-mobile gamma camera combination. *Am J Nucl Med Mol Imaging* 2015; **5**: 233–45.
79. Brouwer OR, van den Berg NS, Mathéron HM, Wendler T, van der Poel HG, Horenblas S, et al. Feasibility of intraoperative navigation to the sentinel node in the groin using preoperatively acquired single photon emission computerized tomography data: transferring functional imaging to the operating room. *J Urol* 2014; **192**: 1810–16. doi: http://dx.doi.org/10.1016/j.juro.2014.03.127
80. Valdes Olmos RA, Vidal-Sicart S, Giammarile F, Zaknun JJ, Van Leeuwen FW, Mariani G. The GOSTT concept and hybrid mixed/virtual/augmented reality environment radioguided surgery. *Q J Nucl Med Mol Imaging* 2014; **58**: 207–15.
81. Brouwer OR, Buckle T, Bunschoten A, Kuil J, Vahrmeijer AL, Wendler T, et al. Image navigation as a means to expand the boundaries of fluorescence-guided surgery. *Phys Med Biol* 2012; **57**: 3123–36. doi: http://dx.doi.org/10.1088/0031-9155/57/10/3123
82. Bluemel C, Herrmann K, Kübler A, Buck AK, Geissinger E, Wild V, et al. Intraoperative 3-D imaging improves sentinel lymph node biopsy in oral cancer. *Eur J Nucl Med Mol Imaging* 2014; **41**: 2257–64. doi: http://dx.doi.org/10.1007/s00259-014-2870-z
83. Buckle T, Kuil J, van den Berg NS, Bunschoten A, Lamb HJ, Yuan H, et al. Use of a single hybrid imaging agent for integration of target validation with *in vivo* and *ex vivo* imaging of mouse tumor lesions resembling human DCIS. *PLoS One* 2013; **8**: e48324. doi: http://dx.doi.org/10.1371/journal.pone.0048324
84. Buckle T, Brouwer OR, Valdés Olmos RA, van der Poel HG, van Leeuwen FW. Relationship between intraprostatic tracer deposits and sentinel lymph node mapping in prostate cancer patients. *J Nucl Med* 2012; **53**: 1026–33. doi: http://dx.doi.org/10.2967/jnumed.111.098517
85. Burggraaf J, Kamerling IM, Gordon PB, Schrier L, de Kam ML, Kales AJ, et al. Detection of colorectal polyps in humans using an intravenously administered fluorescent peptide targeted against c-Met. *Nat Med* 2015; **21**: 955–61. doi: http://dx.doi.org/10.1038/nm.3641
86. van Oosterom MN, Kreuger R, Buckle T, Mahn WA, Bunschoten A, Josephson L, et al. U-SPECT-BioFluo: an integrated radionuclide, bioluminescence, and fluorescence imaging platform. *EJNMMI Res* 2014; **4**: 56. doi: http://dx.doi.org/10.1186/s13550-014-0056-0
87. Grootendorst MR, Kothari A, Cariati M, Cook G, Allen S, Sibley-Allen C, Britten A, et al. Clinical feasibility of intraoperative 18F-FDG Cerenkov Luminescence Imaging in breast cancer surgery. *J Nucl Med* 2015; **56**: 13.